Long-Lived Entanglement Generation of Nuclear Spins Using Coherent Light

Or Katz,[1,2,*] Roy Shaham,[1,2] Eugene S. Polzik,[3] and Ofer Firstenberg[1]
[1]*Department of Physics of Complex Systems, Weizmann Institute of Science, Rehovot 76100, Israel*
[2]*Rafael Ltd, IL-31021 Haifa, Israel*
[3]*Niels Bohr Institute, University of Copenhagen, Blegdamsvej 17, DK-2100 Copenhagen, Denmark*

(Received 24 June 2019; published 29 January 2020)

Nuclear spins of noble-gas atoms are exceptionally isolated from the environment and can maintain their quantum properties for hours at room temperature. Here we develop a mechanism for entangling two such distant macroscopic ensembles by using coherent light input. The interaction between the light and the noble-gas spins in each ensemble is mediated by spin-exchange collisions with alkali-metal spins, which are only virtually excited. The relevant conditions for experimental realizations with ^{3}He or ^{129}Xe are outlined.

DOI: 10.1103/PhysRevLett.124.043602

Quantum entanglement describes correlations between distinct quantum systems and is often used to set borders between the quantum and classical worlds [1,2]. It is a valuable resource for quantum information and computing [3–7] and for metrology beyond the standard quantum limits [8,9]. Generating and maintaining entanglement in matter systems requires exquisite control and isolation, as achieved in ensembles of alkali-metal spins [10–12], trapped ions and atoms [13,14], quantum defects in crystals [15], and high-quality mechanical oscillators [16].

Rare isotopes of noble-gas atoms, such as ^{3}He and ^{129}Xe, have nuclei with nonzero spins. These spins are exceptionally isolated from the environment and can remain coherent for extremely long times, exceeding tens of hours above room temperature [17,18]. Accordingly, the collective nuclear spin of noble-gas ensembles is the longest-living macroscopic quantum object currently known. Nevertheless, while these spin ensembles could potentially maintain entanglement for record times [19,20], they do not interact with optical photons. This limits their applicability for optical quantum communication [10,21–24], or to advanced sensing applications such as hybrid optomechanical-spin systems, e.g., for gravitational-wave detection [25,26]. In 2007, Pinard and coworkers proposed to entangle ^{3}He ensembles using incoherent collisions with metastable ^{3}He atoms and via adiabatic state transfer with nonclassical light in an optical cavity [27]. This pioneering and rather challenging proposal was never realized.

Here we develop a readily feasible scheme for entangling two macroscopic ensembles of noble-gas spins contained in distant cells, as shown in Fig. 1. Our scheme employs the archetypal mechanism for entanglement of spin ensembles, based on continuous measurement of spin fluctuations by off-resonant Faraday rotation of probe light [24]. This mechanism was successfully employed to entangle distant alkali spin ensembles [10]. While there is no direct interaction between light and noble-gas spins, we propose to use auxiliary ensembles of alkali-metal atoms as mediators. The alkali mediators are optically-accessible and couple to the noble-gas spins via coherent spin-exchange collisions [19]. We show that continuous optical measurement of the alkali spins generates a vital entanglement between the noble-gas ensembles. At the same time, dissipation and fluctuations of the alkali spins can be

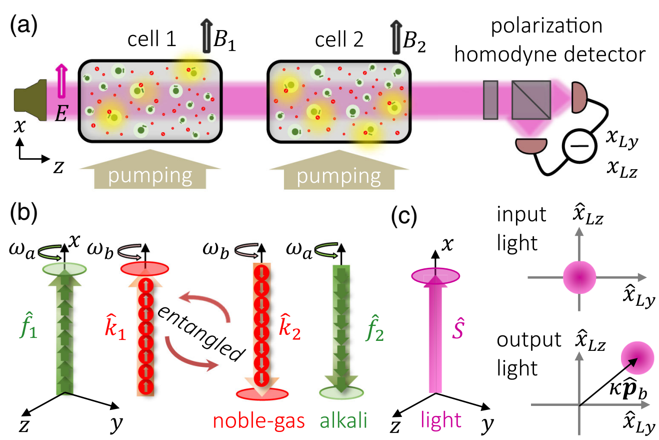

FIG. 1. Entanglement generation of the macroscopic spin-state of two distant noble-gas ensembles. (a) The physical system consists of two cells with mixtures of alkali (green) and noble-gas atoms (red). Homodyne detection of coherent probe light passing through the two cells monitors the correlated spin precession of the noble-gas ensembles. (b) Collective spin states of polarized alkali and noble-gas atoms. The shaded disks denote quantum spin fluctuations. (c) Polarization state of linearly polarized probe, and its rotation via indirect Faraday interaction with the noble-gas spins, as described by Eq. (6). The in-phase $(\hat{x}_{Ly})$ and out-of-phase $(\hat{x}_{Lz})$ components of the probe commute and can be simultaneously measured. Shaded purple disks denote the photon shot noise.

circumvented by introducing a frequency mismatch, such that quantum correlations are mediated without actual excitations of the (alkali) mediators. We outline the physical conditions for experiments with ^{3}He-K and ^{129}Xe-Rb mixtures towards a demonstration of long-lived entanglement of macroscopic systems.

Before diving into the detailed model, we consider a simplified picture of the interaction mechanisms within each cell, presenting the emergence of the Faraday interaction between light and optically inaccessible spins. We describe quantum excitations of the alkali spins by the bosonic operators $\hat{f}, \hat{f}^\dagger$, excitations of noble-gas spins by $\hat{k}, \hat{k}^\dagger$, and the polarization state of probe light by the canonical bosonic operators $\hat{x}_L$ and $\hat{p}_L$. The probe couples to the alkali ground-level spins via the optically excited levels. These levels are subject to rapid relaxation at a rate Γ_e due to spontaneous emission and buffer-gas broadening, leading to spin relaxation and to probe attenuation. Detuning the probe by $|\delta_e| \gg \Gamma_e$ from the optical transition circumvents this relaxation, rendering the atom-photon interaction dispersive. The excited-level spins then adiabatically follow the ground-level spins, yielding the Faraday interaction $\mathcal{H}_{L-a} = i\hbar Q \hat{p}_L(\hat{f}^\dagger - \hat{f})/\sqrt{2}$ between the probe and the alkali spins. $\mathcal{H}_{L-a}$ describes the polarization rotation of far-detuned probe and the resulting alkali-spin rotation at the rate $Q \propto 1/\delta_e$ [11].

The coherent coupling of the alkali spins to the noble-gas spins is described by the exchange Hamiltonian $\mathcal{H}_{a-b} = \hbar J(\hat{f}^\dagger \hat{k} + \hat{k}^\dagger \hat{f})$, where J is the collective exchange rate due to atomic collisions [19]. The resonance conditions for this coupling are governed by the noninteracting Hamiltonian $\mathcal{H}_0 = \hbar\omega_a \hat{f}^\dagger \hat{f} + \hbar\omega_b \hat{k}^\dagger \hat{k}$, where the difference in precession frequencies $\Delta = \omega_a - \omega_b$ is tunable with an external magnetic field.

The alkali spins are prone to fast dephasing at a rate γ_a due to photon absorption, collisions with different atoms and with the cell walls. Here again, the detuning (Δ) determines to what extent this fast alkali relaxation affects the noble-gas spins. On resonance ($|\Delta| \lesssim \gamma_a, J$), the noble-gas spins inherit the alkali-spin relaxation [19], whereas off resonance ($|\Delta| \gg J, \gamma_a$), the interaction is dispersive, suppressing the relaxation induced by the alkali by a factor $\gamma_a/\Delta \ll 1$. The alkali spins then adiabatically follow the noble-gas spins, yielding the overall Hamiltonian $\mathcal{H}_{L-b} = i\hbar Q J \hat{p}_L(\hat{k} - \hat{k}^\dagger)/(\sqrt{2}\Delta)$ in a frame rotating at ω_b when $|\Delta| \gg J$, Q, up to shifts proportional to Q^2/Δ and J^2/Δ. We thus arrive at an indirect Faraday interaction of light with noble-gas spins via virtual excitations of alkali spins.

The concept described above can be applied for entangling two distant noble-gas spin ensembles using probe light and alkali spins [Fig. 1(a)]. Each cell contains N_b noble-gas atoms with spin-1/2, initially polarized along the quantization axis $\boldsymbol{e}_x$. Ensemble $i = 1, (i = 2)$ is polarized upwards $+\boldsymbol{e}_x$ (downwards $-\boldsymbol{e}_x$). Given the spin operators $\hat{\mathbf{k}}_i^{(n)}$ of the nth noble-gas atom in the ith cell, we define the normalized macroscopic spin operator $\hat{\mathbf{k}}_i \equiv M_b^{-1/2} \sum_{n=1}^{N_b} \hat{\mathbf{k}}_i^{(n)}$ for each ensemble. The total magnetization $M_b = P_{mb} N_b/2$ depends on the initial degree of polarization $P_b \leq 1$. For $M_b \gg 1$ and fully polarized ensembles ($P_b = 1$), the initial states are known as coherent spin-states (CSS). A partially polarized ensemble of spin-1/2 atoms may be seen as a mixture of $P_b N_b$ polarized atoms and $(1 - P_b) N_b$ unpolarized atoms, only reducing the coherent interaction strength [11]. The two ensembles have definitive collective spin along $\boldsymbol{e}_x$ with a classical measurement outcome $\langle \hat{\mathrm{k}}_{ix} \rangle = \pm M_b^{1/2}$ and negligible variance, where henceforth the symbol "±" stands for "+" in cell $i = 1$, and for "−" in cell $i = 2$. On the other hand, the transverse components of the normalized collective spin $\hat{\mathrm{k}}_{iy}$ and $\hat{\mathrm{k}}_{iz}$ satisfy the commutation relation $[\hat{\mathrm{k}}_{iy}, \hat{\mathrm{k}}_{jz}] = \pm i\delta_{ij}$ and consequently are governed by quantum fluctuations. These operators are normalized and unitless, giving the collective spin variance in units of vacuum noise. These fluctuations, known as atom-projection noise, are zero on average and have a nonzero variance, satisfying the Robertson inequality $4\mathrm{var}(\hat{\mathrm{k}}_{iy})\mathrm{var}(\hat{\mathrm{k}}_{iz}) \geq |\langle[\hat{\mathrm{k}}_{iy}, \hat{\mathrm{k}}_{iz}]\rangle|^2 = 1$, where $\mathrm{var}(\hat{\mathrm{k}}_{iy}) = \mathrm{var}(\hat{\mathrm{k}}_{iz}) = 1/2$ for CSS. Visually, these fluctuations can be represented as a small uncertainty disk around the classical spin vector, as shown in Fig. 1(b).

Two spin ensembles are entangled if their quantum fluctuations are correlated, as in a two-mode squeezed state. For spins of equal magnitude $|\langle \hat{\mathrm{k}}_{1x} \rangle| = |\langle \hat{\mathrm{k}}_{2x} \rangle|$, a sufficient criterion for EPR-type entanglement is given by [10,28]

$$\mathrm{var}(\hat{\mathrm{k}}_{1y} - \hat{\mathrm{k}}_{2y}) + \mathrm{var}(\hat{\mathrm{k}}_{1z} - \hat{\mathrm{k}}_{2z}) < 2. \tag{1}$$

Therefore, simultaneous measurement of the nonlocal observables $\hat{\mathrm{k}}_{1y} - \hat{\mathrm{k}}_{2y}$ and $\hat{\mathrm{k}}_{1z} - \hat{\mathrm{k}}_{2z}$ generates entanglement, if the total noise variance of the two cells is less than two vacuum-noise units. Such measurement is allowed for oppositely oriented spins $\langle \hat{\mathrm{k}}_{1x} \rangle = -\langle \hat{\mathrm{k}}_{2x} \rangle$, for which $\hat{\mathrm{k}}_{1y} - \hat{\mathrm{k}}_{2y}$ and $\hat{\mathrm{k}}_{1z} - \hat{\mathrm{k}}_{2z}$ commute.

We measure the noble-gas spins using alkali spins and a probe field. Each cell contains N_a alkali atoms, polarized to a polarization degree $P_a \leq 1$ (using auxiliary circularly polarized pump beams) along the same directions $\pm\boldsymbol{e}_x$ as the noble-gas spins. We define for each cell the normalized macroscopic alkali-spin operator $\hat{\mathbf{f}}_i \equiv M_a^{-1/2} \sum_{m=1}^{N_a} \hat{\mathbf{f}}_i^{(m)}$, where $M_a = P_a N_a (I + 1/2)$ is the alkali magnetization, and I is the alkali nuclear spin. Similarly to the noble-gas spins, $\hat{\mathrm{f}}_{ix}$ are considered classical, with $\langle \hat{\mathrm{f}}_{ix} \rangle = \pm M_a^{1/2}$, whereas $\hat{\mathrm{f}}_{iy}$ and $\hat{\mathrm{f}}_{iz}$ are governed by quantum fluctuations. The probe is a square pulse of duration T, propagating along $\boldsymbol{e}_z$ with initial linear polarization $\boldsymbol{e}_x$. We represent its state by the normalized Stokes operators $\hat{\boldsymbol{S}}(z)$ where $\langle \hat{S}_x \rangle^2 = M_L$ is the total number of photons in the pulse, and

$\hat{S}_y, \hat{S}_z$, describe the polarization-state subject to quantum polarization-fluctuations.

The Hamiltonian describing the interactions in the system is given by [10,19]

$$\mathcal{V} = \hbar J(\hat{\mathbf{f}}_1 \cdot \hat{\mathbf{k}}_1 + \hat{\mathbf{f}}_2 \cdot \hat{\mathbf{k}}_2) + \hbar Q(\hat{\mathrm{f}}_{1z} + \hat{\mathrm{f}}_{2z}) \int \frac{dz'}{L} \hat{S}_z(z'). \quad (2)$$

The first term describes a mutual precession of the alkali and noble-gas spins around each other at a rate J. It manifests the coherent collective coupling between these spins via multiple weak spin-exchange collisions [19]. The second term in Eq. (2) describes the dispersive interaction of the alkali spins with the far-detuned probe traversing the two cells [11]. The spin components along the optical axis $(\hat{\mathrm{f}}_{1z} + \hat{\mathrm{f}}_{2z})$ govern the Faraday rotation of the light polarization, while circularly polarized light $(\hat{S}_z)$ acts back to rotate the spins via light shifts. The coupling rate is given by $Q = (a/T)\sqrt{M_a M_L}$, where $a \propto 1/\delta_e$ is the unitless optical-coupling coefficient [11,29] and L is the length of each cell. See the Supplemental Material for detailed expressions of J, Q, and a [30].

To generate entanglement, we set common precession frequencies (ω_a, ω_b) in the two cells, by tuning the magnetic fields and the light-shifts induced by the pumps in each cell [30]. We describe the spin dynamics in a common rotating frame, defined by $\hat{\mathbf{k}}_i \to R_x(\omega_b t)\hat{\mathbf{k}}_i$ and $\hat{\mathbf{f}}_i \to R_x(\omega_b t)\hat{\mathbf{f}}_i$, where $R_x(\theta)$ rotates a vector by an angle θ around $\boldsymbol{e}_x$. In this frame, the alkali spins precess at frequency $\Delta = \omega_a - \omega_b$.

We now take the off-resonance regime $\Delta \gg \gamma_a, J, Q$ and first present the results for negligible relaxations. Given the interaction Hamiltonian (2), we find that the transverse fluctuations $\hat{\mathrm{f}}_{iy}, \hat{\mathrm{f}}_{iz}$ of the alkali spins adiabatically follow the noble-gas spins fluctuations, and the probe polarization,

$$\hat{\mathbf{f}}_i = \pm \frac{J}{\Delta} \hat{\mathbf{k}}_i \pm \frac{Q}{\Delta} \hat{S}_z \boldsymbol{e}(t), \quad (3)$$

where $\boldsymbol{e}(t) = \sin(\omega_b t)\boldsymbol{e}_y + \cos(\omega_b t)\boldsymbol{e}_z$ is the optical axis in the rotating frame. Thus, the large frequency mismatch Δ renders the interaction dispersive, moderating the response of the alkali spins to both spin exchange and backaction of light.

We use Eqs. (2)–(3) to derive the Heisenberg-Langevin equations for the transverse operators $\hat{S}$ and $\hat{\mathbf{k}}_i$ [30]. First, we find that the difference between the noble-gas spins remains constant

$$\partial_t(\hat{\mathbf{k}}_1 - \hat{\mathbf{k}}_2) = 0. \quad (4)$$

Importantly, the preparation of the two cells with oppositely oriented spins eliminates the backaction effect [second term in Eq. (3)] of the probe on the operator $\hat{\mathbf{k}}_1 - \hat{\mathbf{k}}_2$. Second, we find that $\hat{\mathbf{k}}_1 - \hat{\mathbf{k}}_2$ determines the evolution of the probe polarization along the cell

$$\partial_z \hat{S}_y = \frac{QJT}{L\Delta} (\hat{\mathbf{k}}_1 - \hat{\mathbf{k}}_2) \boldsymbol{e}(t). \quad (5)$$

Equation (5) manifests the indirect Faraday interaction between the probe and the noble-gas spins, with the outgoing polarization $\hat{S}_y(L)$ providing a monitor of $\hat{\mathbf{k}}_1 - \hat{\mathbf{k}}_2$. In particular, a simultaneous measurement of the in-phase and out-of-phase components of $\hat{S}_y(L)$ via homodyne detection yields the nonlocal spin components $\hat{\mathrm{k}}_{1y} - \hat{\mathrm{k}}_{2y}$ and $\hat{\mathrm{k}}_{1z} - \hat{\mathrm{k}}_{2z}$, respectively.

The procedure for entanglement generation is shown in Fig. 2. Initially, homodyne measurement of the probe, which underwent the evolution in Eq. (5), drives the noble-gas ensembles to a nonclassical two-mode squeezed state, displaced according to the measurement outcome [11]. Subsequently, feeding back the measurement outcome to rotate the spins (using a short magnetic pulse) sets the mean value of their squeezed components to zero, yielding unconditioned entanglement.

To quantify this process, we define canonical operators for the probe $\hat{\boldsymbol{x}}_L(z) = \sqrt{2}\int_0^T \hat{S}_y(z)\boldsymbol{e}(t)dt/T$ and $\hat{\boldsymbol{p}}_L(z) = \sqrt{2}\int_0^T \hat{S}_z(z)\boldsymbol{e}(t)dt/T$, and nonlocal canonical operators for the noble-gas spins $\hat{\boldsymbol{x}}_b(t) = \boldsymbol{e_x} \times (\hat{\mathbf{k}}_1 + \hat{\mathbf{k}}_2)/\sqrt{2}$ and

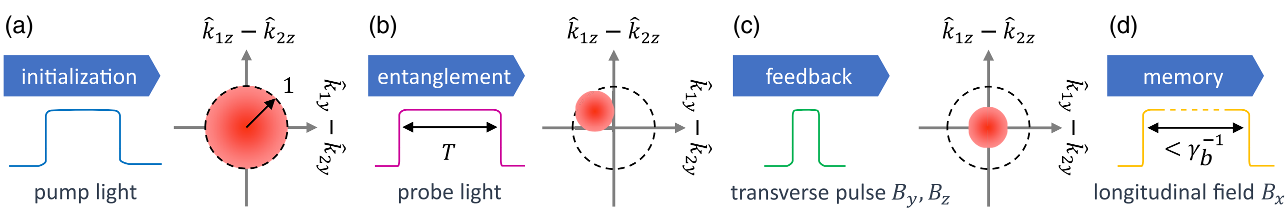

FIG. 2. Sequence for generation and storage of entanglement. (a) The noble-gas ensembles are pumped to coherent spin states with vacuum fluctuations of radius $\mathrm{std}(\hat{k}_{1y} - \hat{k}_{2y}) = \mathrm{std}(\hat{k}_{1z} - \hat{k}_{2z}) = 1$. Dashed circles mark the entanglement criterion from Eq. (1). (b) Homodyne detection of the probe light, via the Faraday interaction [Fig. 1(c)], leads to (conditional) squeezing and displacement of the spin-state. $\hat{k}_{1y} - \hat{k}_{2y}$ and $\hat{k}_{1z} - \hat{k}_{2z}$ commute, and their combined uncertainty can be smaller than 1. (c) A short transverse magnetic-field pulse rotates the spin state, yielding an unconditioned entanglement, satisfying inequality (1). (d) During the memory time, application of a large magnetic-field decouples the noble-gas and alkali spins. The memory lifetime is governed by the long coherence time of the noble-gas spins.

$\hat{\boldsymbol{p}}_b(t) = (\hat{\mathbf{k}}_1 - \hat{\mathbf{k}}_2)/\sqrt{2}$. These constitute two independent Harmonic oscillators. The total evolution is then given by a set of input-output relations, obtained by integration of Eqs. (4)–(5) [30]

$$\hat{\boldsymbol{x}}_L^{\text{out}} = \hat{\boldsymbol{x}}_L^{\text{in}} + \kappa\hat{\boldsymbol{p}}_b^{\text{in}}, \qquad \hat{\boldsymbol{p}}_b^{\text{out}} = \hat{\boldsymbol{p}}_b^{\text{in}}. \tag{6}$$

The input components of the probe $\hat{\boldsymbol{x}}_L^{\text{in}}, \hat{\boldsymbol{p}}_L^{\text{in}}$ comprise the photon shot noise at $z = 0$, and the output components $\hat{\boldsymbol{x}}_L^{\text{out}}, \hat{\boldsymbol{p}}_L^{\text{out}}$ describe the probe state at $z = 2L$ after the cells. Similarly, the noble-gas spin operators $\hat{\boldsymbol{x}}_b^{\text{in}}, \hat{\boldsymbol{p}}_b^{\text{in}}$ comprise the atomic projection noise at $t = 0$, and $\hat{\boldsymbol{x}}_b^{\text{out}}, \hat{\boldsymbol{p}}_b^{\text{out}}$ describe the collective spin state at $t = T$. Therefore, Eqs. (6) describe the Faraday rotation ($\hat{\boldsymbol{x}}_L^{\text{out}}$) of the linearly polarized input light ($\hat{\boldsymbol{x}}_L^{\text{in}}$) by the total noble-gas spin ($\hat{\boldsymbol{p}}_b^{\text{in}}$), as shown in Fig. 1(c), with no backaction ($\hat{\boldsymbol{p}}_b^{\text{out}} = \hat{\boldsymbol{p}}_b^{\text{in}}$). The unitless coupling constant $\kappa \equiv QJT/\Delta$ quantifies the net polarization rotation of the probe. It characterizes the measurement strength of the noble-gas spins with respect to the photon shot-noise, depending on the resonant optical depth of the alkali ensembles [30].

For coherent light and coherent spin-states, the input uncertainties are at the classical minimum, satisfying $\text{var}(\hat{x}_{L,\alpha}^{\text{in}}) = \text{var}(\hat{p}_{L,\alpha}^{\text{in}}) = \text{var}(\hat{x}_{b,\alpha}^{\text{in}}) = \text{var}(\hat{p}_{b,\alpha}^{\text{in}}) = 1/2$ with $\alpha = y, z$. Following the measurement, a magnetic pulse feedback is used for rotating the noble-gas spins from $\hat{\boldsymbol{p}}_b^{\text{out}} = \hat{\boldsymbol{p}}_b^{\text{in}}$ to $\hat{\boldsymbol{p}}_b^{\text{in}} + G\hat{\boldsymbol{x}}_L^{\text{out}}$. The feedback proportionality constant G can be optimally chosen to minimize $\text{var}(\hat{p}_{b,\alpha}^{\text{out}}) = (2 + 2\kappa^2)^{-1}$ for both $\alpha = y, z$. Identifying $\text{var}(\hat{p}_{b,\alpha}^{\text{out}}) = \exp(-2\xi)/2$ as the degree of two-mode squeezing, we obtain the squeezing parameter $\xi = \ln(1 + \kappa^2)/2$. Evidently, any system with $\kappa > 0$ yields nonzero squeezing and satisfies the inequalities $\text{var}(\hat{p}_{b,\alpha}^{\text{out}}) < 1/2$, thus satisfying the entanglement condition in Eq. (1). We therefore conclude that our scheme correlates the spin-states of two distant noble-gas ensembles, generating unconditional entanglement.

We now return to consider relaxation processes expected in realistic conditions. The mechanisms dominating the relaxation rate γ_{sd} of the alkali spin are absorption of probe photons, collisions with noble-gas atoms, spin destruction during alkali collisions, and collisions with the cell walls [19,32–34]. Continuous optical-pumping at a rate R_{op} can be used to maintain a constant alkali magnetization $M_a = P_a N_a(I + 1/2)$, with $P_a = R_{\text{op}}/\gamma_a$ and $\gamma_a = \gamma_{sd} + R_{\text{op}}$. The noble gas is hyperpolarized via spin-exchange optical pumping (SEOP) at a high magnetic field prior to the experiment [32,35]. For polarized alkali spins, the decoherence rate of the noble-gas spins is $\Gamma_b = \gamma_b + (J/\Delta)^2\gamma_a$; it inherits a fraction $(J/\Delta)^2$ of the alkali decoherence rate γ_a, which often dominates Γ_b [36]. At low alkali densities, γ_b is typically limited by technical magnetic inhomogeneities to $\gamma_b \lesssim (\text{minute})^{-1}$ for ^{129}Xe and $\gamma_b \lesssim (\text{hour})^{-1}$ for ^{3}He [17,18,37].

These relaxation processes are accompanied by noise, which increases the measurement variance and limits ξ. We generalize Eqs. (6) and include the relaxation and noise effects, deriving the best attainable two-mode squeezing parameter [30]

$$\xi = \frac{1}{2}\ln\left(\frac{\kappa^2(1-\epsilon)(1+\varrho)+1}{\kappa^2(1-\epsilon)(\eta+\varrho)+1}\right). \tag{7}$$

Here $\epsilon = 4\gamma_L L$ denotes the total fraction of scattered probe photons, $\eta = 2\Gamma_b T$ denotes the fraction of decohered noble-gas spins, and $\varrho = 4q\gamma_a/(J^2 T)$ characterizes the ratio between the contributions of alkali spins and noble-gas spins to the projection noise. The unitless parameter $q(I, P_a) \geq 1$ quantifies the increase of alkali projection-noise (variance) due to imperfect spin-polarization, where $q(0, P_a) = q(I, 1) = 1$ [29]. Equation (7) guarantees the generation of entanglement between the two ensembles for $\eta \ll 1$. Notably, it has the same form as for squeezing two alkali ensembles [11] except for the additional parameter ϱ. In Fig. 3, we use Eq. (7) to plot the degree of squeezing $\exp(-2\xi)$ of the two noble-gas spin-ensembles as a function of $\kappa\sqrt{1-\epsilon}$ and ϱ for two values of η.

Our entanglement generation scheme can be realized with various alkali and noble-gas mixtures within a large range of experimental parameters. Here we present a representative configuration for entangling two ^{3}He ensembles in two cylindrical cells of length $L = 5$ cm and cross section $A = 2\ \text{mm}^2$. We consider a gaseous mixture of 880 Torr ^{3}He, 70 Torr N_2, and a droplet of K at 250 °C. Here $R_{\text{op}} = 1.6\gamma_a$ yields $P_a = 0.62$ [with $q(3/2, P_a) = 1.22$] and $P_b = 0.56$, assuming $\gamma_b^{-1} = 50$ hour. The 400-mW probe is detuned 3 THz from the optical line, and $B_1 \approx 10$ mG. Homodyne detection for $T = 200$ msec

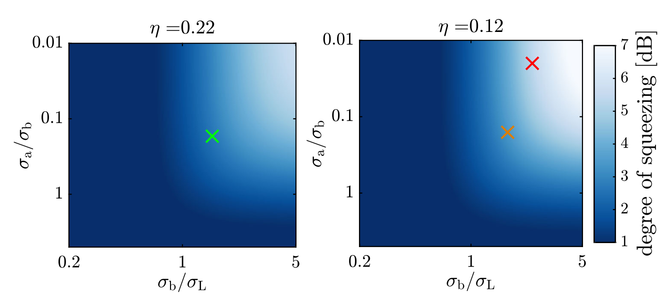

FIG. 3. Attainable degree of two-mode spin squeezing for noble-gas ensembles. We present results for both $\eta = 0.22$ and $\eta = 0.12$, where η characterizes the fractional decoherence of the noble-gas spins during the entangling process. The parameters σ_a, σ_b, and σ_L denote the contributions of the alkali spin-projection noise, noble-gas spin-projection noise, and photon shot noise, respectively, to the optical measurements. The squeezing is maximized when the noble-gas noise σ_b dominates the measurement. The calculations are done using Eq. (7), with $\sigma_b/\sigma_{mL} = \kappa\sqrt{1-\epsilon}$ and $\sigma_a/\sigma_b = \varrho$. The crosses mark proposed working points with ^{129}Xe-^{87}Rb (green) and ^{3}He-K (red, orange).

yields $\kappa = 2$, $\epsilon = 0.3$, $\eta = 0.125$, and $\varrho = 0.162$, generating 4 dB of two-mode squeezing ($\xi = 0.45$), which could live for tens of hours. The performance for this configuration is marked in Fig. 3 (orange cross). Other exemplary experimental configurations, marked in Fig. 3 and detailed in [30], yield 6 dB of squeezing for ^{3}He-K mixture (red cross) and 3 dB of squeezing for ^{129}Xe-^{87}Rb mixture (green cross).

The long coherence time within each noble-gas spin ensemble ideally also applies to the entanglement lifetime, even though each ensemble comprises a macroscopic number of spins. In the Holstein-Primakoff approximation, the number of spin excitations is independent of the total number of spins. Indeed we show in [30] that the squeezed quadrature, $\mathrm{var}(\hat{\boldsymbol{p}}_b^{\mathrm{out}}) < 1/2$, decays at a constant rate $2\Gamma_b$.

The long-lived entanglement can be verified by applying an off-resonant probe pulse, measuring the two spin-ensembles simultaneously by utilizing the same experimental configuration used for their generation [10]. Alternatively, the spin of each cell could be measured independently, and their cross-correlations can be found. In systems featuring strong coupling between the alkali and noble gas ($J \gg \gamma_a$), as was recently observed for a K-^{3}He mixture [38], setting $\Delta = 0$ by tuning the magnetic-field enables efficient transfer of the entanglement to the alkali ensembles. Transfer times J^{-1} of a few milliseconds are possible [19], realizing fast operations yet maintaining long coherence times. The alkali squeezed state could then be projected using a short probe pulse.

In summary, we presented a scheme for entangling the collective nuclear spins of two macroscopic noble-gas ensembles, relying on alkali spin for obtaining an indirect Faraday interaction between the noble-gas and light. The role of relaxations has been considered, revealing that sizable degree of entanglement can be generated at standard experimental conditions, and maintained for extremely long times. With the technologically available, miniature cells [39–41], exceptionally long coherence times, and the entanglement of hot spin ensembles hold a promise for realizing new quantum-optics applications and enhanced sensing at ambient conditions. The scheme could potentially be extended to generate entanglement in other physical systems having hybrid electronic and optically inaccessible nuclear spins, including quantum dots, diamond color centers, and rare earth impurities interacting with nearby nuclear spins in the crystal.

We acknowledge financial support by the ERC starting investigator Grant No. Q-PHOTONICS 678674, ERC Advanced Grant No. QUANTUM-N, the Israel Science Foundation and ICORE, the Pazy Foundation, the Minerva Foundation with funding from the Federal German Ministry for Education and Research, and the Laboratory in Memory of Leon and Blacky Broder. E. S. P. was supported by VILLUM FONDEN under a Villum Investigator Grant, Grant No. 25880.

*or.katz@weizmann.ac.il

[1] S. Haroche, Phys. Today **51**, No. 7, 36 (1998).
[2] R. Horodecki, P. Horodecki, M. Horodecki, and K. Horodecki, Rev. Mod. Phys. **81**, 865 (2009).
[3] M. A. Nielsen and I. L. Chuang, *Quantum Computation and Quantum Information* (Cambridge University Press, Cambridge, UK, 2000).
[4] T. D. Ladd, F. Jelezko, R. Laflamme, Y. Nakamura, C. Monroe, and J. L. O'Brien, Nature (London) **464**, 45 (2010).
[5] S. L. Braunstein and P. van Loock, Rev. Mod. Phys. **77**, 513 (2005).
[6] N. Gisin and R. Thew, Nat. Photonics **1**, 165 (2007).
[7] H. J. Kimble, Nature (London) **453**, 1023 (2008).
[8] L. Pezzé, A. Smerzi, M. K. Oberthaler, R. Schmied, and P. Treutlein, Rev. Mod. Phys. **90**, 035005 (2018).
[9] W. Wasilewski, K. Jensen, H. Krauter, J. J. Renema, M. V. Balabas, and E. S. Polzik, Phys. Rev. Lett. **104**, 133601 (2010).
[10] B. Julsgaard, A. Kozhekin, and E. S. Polzik, Nature (London) **413**, 400 (2001).
[11] K. Hammerer, A. S. Sørensen, and E. S. Polzik, Rev. Mod. Phys. **82**, 1041 (2010).
[12] J. Kong, R. Jiménez-Martínez, C. Troullinou, V. G. Lucivero, and M. W. Mitchell, arXiv:1804.07818.
[13] H. Häffner *et al.*, Nature (London) **438**, 643 (2005).
[14] I. Bloch, Nature (London) **453**, 1016 (2008).
[15] P. Neumann, N. Mizuochi, F. Rempp, P. Hemmer, H. Watanabe, S. Yamasaki, V. Jacques, T. Gaebel, F. Jelezko, and J. Wrachtrup, Science **320**, 1326 (2008).
[16] A. D. O'Connell *et al.*, Nature (London) **464**, 697 (2010).
[17] C. Gemmel *et al.*, Eur. Phys. J. D **57**, 303 (2010).
[18] T. R. Gentile, P. J. Nacher, B. Saam, and T. G. Walker, Rev. Mod. Phys. **89**, 045004 (2017).
[19] O. Katz, R. Shaham, and O. Firstenberg, arXiv:1905.12532.
[20] A. Dantan, G. Reinaudi, A. Sinatra, F. Laloë, E. Giacobino, and M. Pinard, Phys. Rev. Lett. **95**, 123002 (2005).
[21] A. Kuzmich, K. Mölmer, and E. S. Polzik, Phys. Rev. Lett. **79**, 4782 (1997).
[22] A. Kuzmich, L. Mandel, and N. P. Bigelow, Phys. Rev. Lett. **85**, 1594 (2000).
[23] A. Kuzmich and E. S. Polzik, Phys. Rev. Lett. **85**, 5639 (2000).
[24] L. M. Duan, J. I. Cirac, P. Zoller, and E. S. Polzik, Phys. Rev. Lett. **85**, 5643 (2000).
[25] C. B. Møller, R. A. Thomas, G. Vasilakis, E. Zeuthen, Y. Tsaturyan, K. Jensen, A. Schliesser, K. Hammerer, and E. S. Polzik, Nature (London) **547**, 191 (2017).
[26] E. Zeuthen, E. S. Polzik, and F. Y. Khalili, Phys. Rev. D **100**, 062004 (2019).
[27] G. Reinaudi, A. Sinatra, A. Dantan, and M. Pinard, J. Mod. Opt. **54**, 675 (2007).
[28] L. M. Duan, G. Giedke, J. I. Cirac, and P. Zoller, Phys. Rev. Lett. **84**, 2722 (2000).
[29] G. Vasilakis, V. Shah, and M. V. Romalis, Phys. Rev. Lett. **106**, 143601 (2011).
[30] See Supplemental Material at http://link.aps.org/supplemental/10.1103/PhysRevLett.124.043602 for the derivation of the equations of motion, analysis of the entanglement lifetime, presentation of additional experimental

configurations, and derivation of optical depth as a resource for entanglement generation, which includes Ref. [31].

[31] S. M. Rochester, D. S. Hsiung, D. Budker, R. Y. Chiao, D. F. Kimball, and V. V. Yashchuk, Phys. Rev. A **63**, 043814 (2001).

[32] W. Happer, Y. Y. Jau, and T. Walker, *Optically Pumped Atoms* (Wiley-VCH Press, Weinheim Germany, 2010), pp. 15–218.

[33] O. Katz, O. Peleg, and O. Firstenberg, Phys. Rev. Lett. **115**, 113003 (2015).

[34] O. Katz and O. Firstenberg, Nat. Commun. **9**, 2074 (2018).

[35] W. Happer, E. Miron, S. Schaefer, D. Schreiber, W. A. van Wijngaarden, and X. Zeng, Phys. Rev. A **29**, 3092 (1984).

[36] T. W. Kornack and M. V. Romalis, Phys. Rev. Lett. **89**, 253002 (2002).

[37] X. Zeng, Z. Wu, T. Call, E. Miron, D. Schreiber, and W. Happer, Phys. Rev. A **31**, 260 (1985).

[38] R. Shaham, O. Katz, and O. Firstenberg, Strong Coherent Coupling to Noble-Gas Spins (unpublished), http://www.weizmann.ac.il/complex/Firstenberg/noble_strong_coupling.

[39] M. E. Limes, N. Dural, M. V. Romalis, E. L. Foley, T. W. Kornack, A. Nelson, L. R. Grisham, and J. Vaara, Phys. Rev. A **100**, 010501(R) (2019).

[40] T. G. Walker and M. S. Larsen, Adv. At. Mol. Opt. Phys. **65**, 373 (2016).

[41] D. A. Thrasher, S. S. Sorensen, and T. G. Walker, arXiv:1912.04991.